

Early Solar System Solar Wind Implantation of ${}^7\text{Be}$ into Calcium-Aluminum Rich Inclusions in Primitive Meteorites

Glynn E. Bricker

Department of Physics, Purdue University Northwest, Westville, USA

Email: gbricker@pnw.edu

How to cite this paper: Bricker, G.E. (2019) Early Solar System Solar Wind Implantation of ${}^7\text{Be}$ into Calcium-Aluminum Rich Inclusions in Primitive Meteorites. *International Journal of Astronomy and Astrophysics*, 9, 12-20.

<https://doi.org/10.4236/ijaa.2019.91002>

Received: November 27, 2018

Accepted: January 21, 2019

Published: January 24, 2019

Copyright © 2019 by author(s) and Scientific Research Publishing Inc. This work is licensed under the Creative Commons Attribution International License (CC BY 4.0).

<http://creativecommons.org/licenses/by/4.0/>



Open Access

Abstract

The one time presence of short-lived radionuclides (SLRs) in Calcium-Aluminum Rich inclusions (CAIs) in primitive meteorites has been detected. The solar wind implantation model (SWIM) is one possible model that attempts to explain the catalogue of SLRs found in primitive meteorites. In the SWIM, solar energetic particle (SEP) nuclear interactions with gas in the proto-solar atmosphere of young stellar objects (YSOs) give rise to daughter nuclei, including SLRs. These daughter nuclei then may become entrained in the solar wind via magnetic field lines. Subsequently, the nuclei, including SLRs, may be implanted into CAI precursors that have fallen from the main accretion flow which had been destined for the proto-star. This mode of implanting SLRs in the solar system is viable, and is exemplified by the impregnation of the lunar surface with solar wind particles, including SLRs. X-ray luminosities have been measured to be 100,000 times more energetic in YSOs, including T-Tauri stars, than present-day solar luminosities. The SWIM scales the production rate of SLRs to nascent SEP activity in T-Tauri stars. Here, we model the implantation of ${}^7\text{Be}$ into CAIs in the SWIM, utilizing the enhanced SEP fluxes and the rate of refractory mass inflowing at the X-region, 0.06 AU from the proto-Sun. Taking into account the radioactive decay of ${}^7\text{Be}$ and spectral flare variations, the ${}^7\text{Be}/{}^9\text{Be}$ initial isotopic ratio is found to range from 1×10^{-5} to 5×10^{-5} .

Keywords

Radio-Nuclide, ${}^7\text{Be}$, Early Solar System, Solar Wind, CAI, Solar Wind Implantation Model, X-Wind

1. Introduction

Studies report evidence for the one-time presence of SLRs, through decay prod-

uct systematics, including ^{10}Be , ^{26}Al , ^{36}Cl , ^{41}Ca , and ^{53}Mn , in CAIs in primitive carbonaceous meteorites at the nascence of the solar system [1]. The possible origins of these SLRs are widely varied and include stellar sources (AGB Stars, Wolf-Rayet stars, nova, and super nova) and energetic particle interaction, from either SEPs, or galactic cosmic rays (GCRs). Bricker & Caffee [2] [3] proposed the solar wind implantation model (SWIM) for the incorporation of ^{10}Be and ^{36}Cl into CAIs early in primitive meteorites.

In the SWIM, the SLRs come into existence via SEP nuclear reactions in the proto-solar atmosphere of the young Sun, characterized by X-ray emissions orders of magnitude greater than main sequence stars. Studies of the Orion Nebulae indicate that pre-main sequence (PMS) stars exhibit X-ray luminosity, and hence SEP fluxes on the order of $\sim 10^5$ over contemporary SEP flux levels [4]. The irradiation produced SLRs are then trapped by magnetic field lines, and these solar wind SLRs eventually impregnate CAI precursors. This mode of production of SLRs, entrainment of SLRs in the solar wind, and implantation of SLR into solar system material is seen in the implantation of solar wind particles, e.g. ^{10}Be [5] [6] and ^{14}C [6] [7], on the Moon.

^{10}Be is produced via SEP spallation reactions, with oxygen serving as the chief target particle in the SWIM. Similar to ^{10}Be , ^7Be , half-life of 53 days [8], is also primarily produced through SEP nuclear reactions with oxygen as the primary target particle, and ^7Be has also recently been detected in stellar photospheres [9]. In addition, the one-time presence of ^7Be has been measured in CAIs in primitive meteorites (through the study of Li, the decay product of ^7Be , systematics) [10] [11]. Owing to the 53 day half-life, local irradiation is the only possible operation pathway for ^7Be production. As such, the large difference in half-lives between ^7Be and ^{10}Be is of interest in terms of chronological processes associated with early solar system and CAI formation and evolution.

In this work, we consider the possible incorporation of ^7Be into CAIs in primitive carbonaceous meteorites in the SWIM. **Table 1** below characterizes beryllium isotopes found in CAIs.

2. Solar Wind Implantation Mode

2.1. Synopsis

In the SWIM, SLRs are produced in the solar nebula via SEP nuclear reactions on gaseous target material in the solar atmosphere ~ 4.6 Gyr, during the formation

Table 1. Beryllium isotopes found in CAIs.

Nuclide	Half-life	Initial Isotopic Ratio	Radionuclide (g^{-1})
^7Be	53 days [8]	1.2×10^{-3} [10]	1.0×10^{13}
		6.1×10^{-3} [11]	5.3×10^{13}
^{10}Be	1.36×10^6 yr [12]	9.5×10^{-4} [13]	6.4×10^{12}

Note: Radionuclide content in g^{-1} calculated from initial isotopic ratio and ^9Be content in ppb. The ^9Be content in CAIs is estimated 100 ppb [14] [15].

of the solar system. These newly produced nuclei are incorporated in the solar wind. The SLRs flow along magnetic field lines in the solar wind, and this particle flow intersects with materials which have fallen out of the main accretion flow, which was headed to hot-spots on the Sun. At the intersection of outflowing SLRs, and inflowing fallen CAI precursor material, the SLRs may become impregnated into the inflowing materials. The fundamental geometry for the implantation process described above and transportation of implanted CAIs to the asteroid zone can be gleaned from the X-wind model of Shu *et al.* [16] [17] [18]. **Figure 1** below illustrates of the basic magnetic field geometry, ${}^7\text{Be}$ production via SEP flaring activity, and subsequent implantation into CAI-precursor material from the main funnel flow onto the proto-Sun.

2.2. Refractory Mass Inflow Rate

The effective refractory mass inflow rate, S , *i.e.* the refractory mass that falls from the main funnel flow which was accreting onto the star at the X-region, is calculated from equation (1):

$$S = \dot{M}_D \cdot X_r \cdot F \quad (1)$$

where \dot{M}_D is disk mass accretion rate, X_r is the cosmic mass fraction, and F is the fraction of material that enters the X-region from the main funnel flow [19]. For \dot{M}_D , we adopt 1×10^{-7} solar masses year $^{-1}$. Disk mass accretion rates range from $\sim 10^{-7}$ to $\sim 10^{-10}$ solar masses year $^{-1}$ for T Tauri stars from 1 - 3 Myr [20], whereas embedded class 0 and class I PMS stars have mass accretion rates of $\sim 10^{-5}$ to $\sim 10^{-6}$ solar masses year $^{-1}$ [21]. Here we adopt for \dot{M}_D , a rate 1×10^{-7} solar masses year $^{-1}$, corresponding to class II or III PMS stars. From Lee *et al.* [19] we utilize a cosmic mass fraction, X_r , and fraction of refractory material fraction F , of 4×10^{-3} and 0.01, respectively, in our model. X_r represents the fraction of refractory content in the inflowing material, and F represents the fraction of inflowing mass that does not accrete onto the proto-sun. The choice 0.01

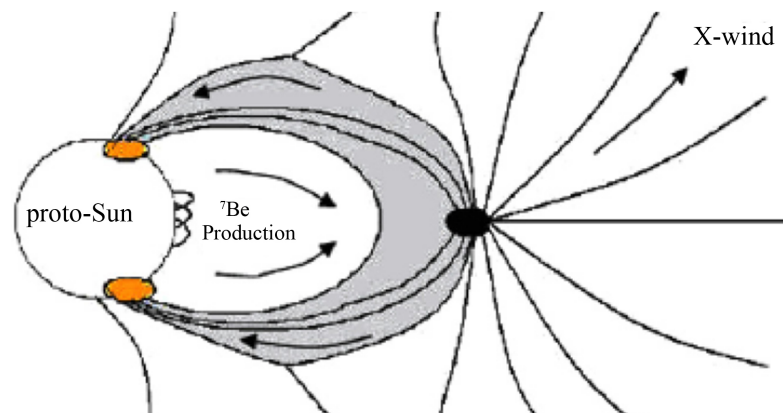


Figure 1. SWIM magnetic field geometry for SLRs production via SEP nuclear reactions. The gray area represents the main accretion flow onto “hot spots” on the PMS star. SLRs produced close to the proto-solar surface are incorporated into CAI precursor material which has fallen from the accretion flow (figure after Shu *et al.* [17]).

maximizes F , and corresponds to all the mass which comprises the planets falling from the accretion flow. $F = 0.01$ is the preferred value of Lee *et al.* [19] in their model. (See Lee *et al.* [19] for a detailed discussion of X , and F) Employing Equation (1) and the parameters detailed above, we find the rate at which this refractory material reaches the x-region, called here the refractory mass inflow rate, S , is $2.5 \times 10^{14} \text{ g s}^{-1}$. In consideration of the extreme values of, S , S could be two orders of magnitude greater if the accretion rates of $\sim 10^{-5}$ to $\sim 10^{-6}$ solar masses year^{-1} , or S could also be four orders of magnitude less if the mass accretion rate was $\sim 10^{-8}$ to 10^{-10} solar masses year^{-1} and $F \sim 0.0001$.

2.3. Effective Ancient Production Rate

The effective ancient ${}^7\text{Be}$ outflow rate, P in units of s^{-1} , is given by:

$$P = p \cdot f \quad (2)$$

where p is the ancient production rate and f is the fraction of the solar wind ${}^7\text{Be}$ that enters the CAI-forming region; $f = 0.1$. (See Bricker & Caffee [2] [3] for a discussion of factor f). The ${}^7\text{Be}$ production rate is calculated assuming that SEPs are characterized by a power law relationship:

$$\frac{dF}{dE} = kE^{-r} \quad (3)$$

where r ranges from 2.5 to 4. For impulsive flares, *i.e.* $r = 4$, we use ${}^3\text{He}/\text{H} = 0.1$ and ${}^3\text{He}/\text{H} = 0.3$, and for gradual flares, *i.e.* $r = 2.5$, we use ${}^3\text{He}/\text{H} = 0$. For all spectral indices, we assume $a/\text{H} = 0.1$. Contemporary SEP flux rates at the Sun-Earth distance of 1 AU are ~ 100 protons $\text{cm}^{-2}\cdot\text{s}^{-1}$ for $E > 10$ MeV [22]. We assume an increase in ancient particle fluxes over the current particle flux of $\sim 4 \times 10^5$ [2] [4], yielding an energetic particle flux rate of 3.7×10^{12} protons $\text{cm}^{-2}\cdot\text{s}^{-1}$ for $E > 10$ MeV at the surface of the proto-Sun.

The production rates for cosmogenic nuclides can be calculated via:

$$p = \sum_i N_i \int \sigma_{ij} \frac{dF(E)}{dE_j} dE \quad (4)$$

where i represents the target elements for the production of the considered nuclide, N_i is the abundance of the target element ($\text{g}\cdot\text{g}^{-1}$), j indicates the energetic particles that cause the reaction, $\sigma_{ij}(E)$ is the cross section for the production of the nuclide from the interaction of particle j with energy E from target i for the considered reaction (cm^2), and $\frac{dF(E)}{dE_j} dE$ is the differential energetic particle flux of particle j at energy E ($\text{cm}^{-2}\cdot\text{s}^{-1}$) [22]. We assume gaseous oxygen target particles of solar composition [23].

The cross-section we use to calculate ${}^7\text{Be}$ production from protons and ${}^4\text{He}$ pathways is from Sisterson *et al.* [24], and the cross-section we use for production from ${}^3\text{He}$ is from Gounelle *et al.* [25]. The Sisterson *et al.* [24] cross-section is experimental obtained, and the Gounelle *et al.* [25] cross-section is a combination of experimental data, fragmentation and Hauser-Feshbach codes. The un-

certainty associated with model codes are at best a factor of two. Taking into account both target abundance and nuclear cross-sections, the reaction with oxygen as the target is the primary production pathway. Any other nuclear reaction would add little to the overall ${}^7\text{Be}$ production rate. **Table 2** shows the nuclear reactions considered in the calculations.

3. Results

The content of ${}^7\text{Be}$ found in refractory material, in atoms g^{-1} , predicted by SWIM is given by:

$$N^{7\text{Be}} = \frac{P}{S} = \frac{P \cdot f}{\dot{M}_D \cdot X_r \cdot F} \quad (5)$$

where P is given atoms s^{-1} and S is given in $\text{g} \cdot \text{s}^{-1}$.

Using the refractory mass inflow rate, S , of $2.5 \times 10^{14} \text{ g} \cdot \text{s}^{-1}$ from Equation (1), and calculations of P , the effective ancient ${}^7\text{Be}$ outflow rate, from Equation (2) & Equation (4), we determine the content of ${}^7\text{Be}$ in CAIs in atoms g^{-1} using Equation (5), and find the associated isotopic ratio for different flare parameters given in **Table 3**. **Figure 2** depicts the ${}^7\text{Be}$ isotopic ratio predicted by the SWIM from SEPs.

4. Discussion

Similar to ${}^{10}\text{Be}$, the primary target for SEP production of ${}^7\text{Be}$ is oxygen. As such, the SEP origin of ${}^7\text{Be}$ and ${}^{10}\text{Be}$ are uniquely intertwined. The estimated ${}^7\text{Be}/{}^{10}\text{Be}$ production ratio from MeV SEPs in the early solar system is estimated to be ~ 70 [14]. Using the production rate from Equation (4) and the production rate for ${}^{10}\text{Be}$ from Bricker & Caffee [2] from SEP interaction with oxygen targets, we obtain a production ratio of ~ 50 , which is similar to Leya [14]. It would then be expected that the original ratio of ${}^7\text{Be}/{}^9\text{Be}$ found in CAIs would be ~ 50 times greater than the ${}^{10}\text{Be}/{}^9\text{Be}$ ratio, assuming the simple SWIM mechanism described above. Using 9.5×10^{-4} [13] as the canonical ${}^{10}\text{Be}/{}^9\text{Be}$ ratio, the ${}^7\text{Be}/{}^9\text{Be}$ ratio would scale to 4.8×10^{-2} . We find this ratio is reproducible within a factor of ~ 5 , the uncertainty associated with SWIM, for spectral indices $r > 3.2$. The SWIM can account for the scaled up ${}^7\text{Be}/{}^9\text{Be}$ ratio. **Figure 3** below details the ratio of ${}^7\text{Be}/{}^9\text{Be}$ from SWIM to 4.8×10^{-2} .

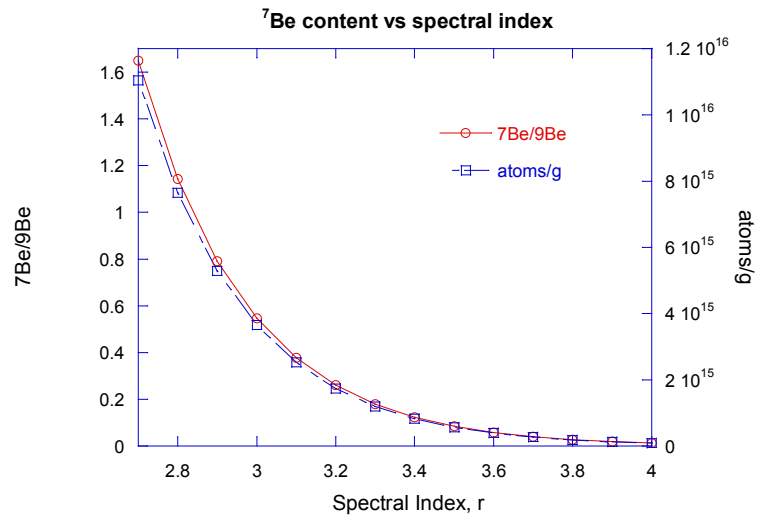
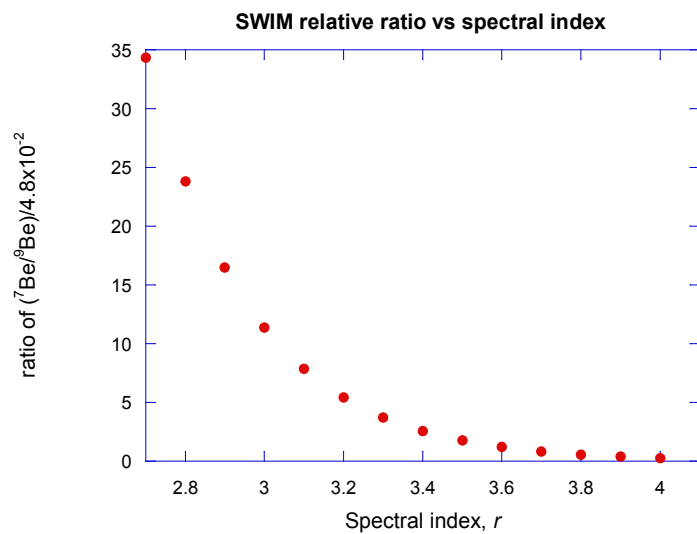
Experimentally obtained measurements for the original ${}^7\text{Be}/{}^9\text{Be}$ ratio in CAIs are limited and a matter of considerable debate. Limited experimentally determined values for the ratio range from about 1.2×10^{-3} [11] to 6.1×10^{-3} [10]. The experimentally obtained ratios are at least a factor of 10 less than SWIM

Table 2. Nuclear reactions considered in this paper.

${}^{16}\text{O}(p, x){}^7\text{Be}$
${}^{16}\text{O}({}^3\text{He}, x){}^7\text{Be}$
${}^{16}\text{O}({}^4\text{He}, x){}^7\text{Be}$

Table 3. Predicted ${}^7\text{Be}$ content in CAIs.

Flare Parameter	atoms g^{-1} (in CAIs)	Isotopic Ratio
$p = 2.7, {}^3\text{He}/\text{H} = 0$	1.1×10^{16}	1.6
$p = 4, {}^3\text{He}/\text{H} = 0.1$	3.8×10^{14}	5.7×10^{-2}
$p = 4, {}^3\text{He}/\text{H} = 0.3$	1.1×10^{15}	1.6×10^{-1}

**Figure 2.** Predicted ${}^7\text{Be}$ content in CAIs from energetic protons as a function of solar flare parameter.**Figure 3.** Ratio of ${}^7\text{Be}/{}^9\text{Be}$ found from SWIM. A ratio of one indicates exact match, a ratio greater than one indicates overproduction, and a ratio less than one indicates underproduction.

calculations, and also a factor of at least 10 less than the scaled up ${}^7\text{Be}/{}^9\text{Be}$ found from scaling the canonical ${}^{10}\text{Be}/{}^9\text{Be}$ ratio to ${}^7\text{Be}$ and ${}^{10}\text{Be}$ production rates. **Figure 4** depicts the ratio of SWIM obtained ratio to the canonical ${}^7\text{Be}/{}^9\text{Be}$ ratio.

Clearly, some other mechanism is needed to explain the overproduction of the

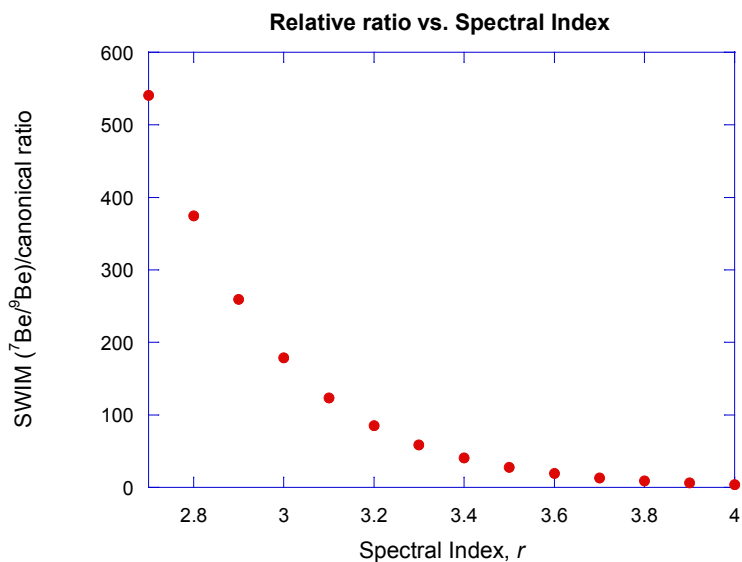


Figure 4. Ratio of SWIM ${}^9\text{Be}/{}^{10}\text{Be}$ ratio to canonical ${}^7\text{Be}/{}^9\text{Be}$ ratio. A factor greater than one indicates overproduction relative to canonical.

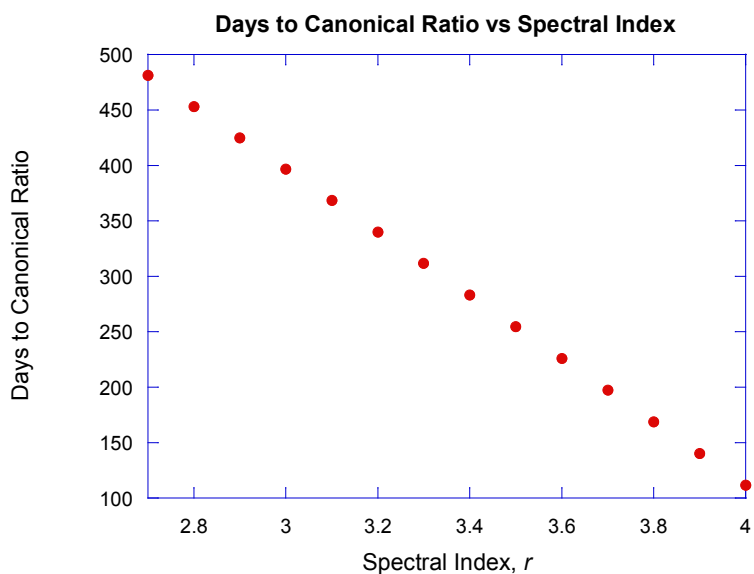


Figure 5. Days to canonical ratio vs. spectral index.

${}^7\text{Be}/{}^9\text{Be}$ ratio, both in terms of SWIM calculations and the scaling of the ${}^{10}\text{Be}/{}^9\text{Be}$ to relative ${}^7\text{Be}$ and ${}^{10}\text{Be}$ production rates.

An assumption of SWIM is that radionuclides are produced via SEP interaction and then immediately incorporated into CAI precursor materials. With a half-life of 53 days, it is possible that some temporal evolution occurs before ${}^7\text{Be}$ becomes implanted. **Figure 5** shows days to canonical ratio for spectral index.

Figure 5 shows that with a delay on the order of ~ 100 days from the time of production of ${}^7\text{Be}$ to implantation in to CAI precursor materials, the canonical ratio is replicated. Taking into account the time from production of the radio-

nuclide to implantation into CAI precursors, *i.e.*, two half-lives of ${}^7\text{Be}$, explains the deficit in ${}^7\text{Be}/{}^{10}\text{Be}$ measured ratio in comparison to the ${}^7\text{Be}/{}^{10}\text{Be}$ production ratio. It is possible and likely for nuclei to have some finite residence time in the photosphere. Calculations of this residence time have not been performed and are beyond the scope of this paper. Our *ad hoc* choice of two half-lives of residence time for ${}^7\text{Be}$ was to explain the ${}^7\text{Be}/{}^{10}\text{Be}$ measured ratio in comparison to the ${}^7\text{Be}/{}^{10}\text{Be}$ production ratio.

Conflicts of Interest

The author declares no conflicts of interest regarding the publication of this paper.

References

- [1] Gounelle, M., Chaussidon, M. and Montmerle, T. (2007) Irradiation in the Early Solar System and the Origin of Short-Lived Radionuclides. *Comptes Rendus Geoscience*, **339**, 885-894. <https://doi.org/10.1016/j.crte.2007.09.016>
- [2] Bricker, G.E. and Caffee, M.W. (2010) Solar Wind Implantation Model for ${}^{10}\text{Be}$ in CAIs. *Astrophysical Journal*, **725**, 443-449. <https://doi.org/10.1088/0004-637X/725/1/443>
- [3] Bricker, G.E. and Caffee, M.W. (2013) Incorporation of ${}^{36}\text{Cl}$ in Calcium-Aluminum-Rich Inclusions in the Solar Wind Implantation Model. *Advances in Astronomy*, **2013**, Article ID: 487606. <https://doi.org/10.1155/2013/487606>
- [4] Feigelson, E.D., Garmire, G.P. and Pravdo, S.H. (2002) Magnetic Flaring in the Pre-Main-Sequence Sun and Implications for the Early Solar System. *Astrophysical Journal*, **572**, 335-349. <https://doi.org/10.1086/340340>
- [5] Nishiizumi, K. and Caffee, M.W. (2001) Beryllium-10 from the Sun. *Science*, **294**, 352-354. <https://doi.org/10.1126/science.1062545>
- [6] Bricker, G.E. (2013) Calculation of ${}^{10}\text{Be}$ and ${}^{14}\text{C}$ in the Solar Atmosphere: Implication for Solar Flare Spectral Index. *International Journal of Astronomy and Astrophysics*, **3**, 17-20. <https://doi.org/10.4236/ijaa.2013.32A003>
- [7] Jull, A.J.T., Lal, D., McHargue, L.R., Burr, G.S. and Donahue, D.J. (2000) Cosmogenic and Implanted Radionuclides Studied by Selective Etching of Lunar Soils. *Nuclear Instruments & Methods in Physics Research Section B*, **172**, 867-872. [https://doi.org/10.1016/S0168-583X\(00\)00232-9](https://doi.org/10.1016/S0168-583X(00)00232-9)
- [8] Jaeger, M., Wilmes, S., Kölle, V., Staudt, G. and Mohr, P. (1996) Precision Measurement of the Half-Life of ${}^7\text{Be}$. *Physical Review*, **C54**, 423-424. <https://doi.org/10.1103/PhysRevC.54.423>
- [9] Mandzhavidz, N., Ramaty, R. and Kozlovsky, B. (1997) Solar Atmospheric and Solar Flare Accelerated Helium Abundances from Gamma-Ray Spectroscopy. *Astrophysical Journal*, **489**, L99-L102. <https://doi.org/10.1086/310965>
- [10] Chaussidon, M., Robert, F. and McKeegan, K. (2006) Li and B Isotopic Variations in an Allende CAI: Evidence for the *In Situ* Decay of Short-Lived ${}^{10}\text{Be}$ and for the Possible Presence of the Short-Lived Nuclide ${}^7\text{Be}$ in the Early Solar System. *Geochimica et Cosmochimica Acta*, **70**, 224-225. <https://doi.org/10.1016/j.gca.2005.08.016>
- [11] Mishra, R. and Marhas, K. (2018) Fossil Record of ${}^7\text{Be}$ and ${}^{10}\text{Be}$ in a Cai: Implications for the Origin and Early Evolution of Our Solar System. *81st Annual Meeting*

of the Meteoritical Society, Moscow, 22-27 July 2018, Article ID: 6125.

- [12] Nishiizumi, K., Imamura, M., Caffee, M., Southon, J., Finkel, R. and McAnich, J. (2007) Absolute Calibration of ^{10}Be AMS Standards. *Nuclear Instruments and Methods in Physics Research B: Beam Interactions with Materials and Atoms*, **258**, 403-413. <https://doi.org/10.1016/j.nimb.2007.01.297>
- [13] McKeegan, K., Chaussidon, M. and Robert, F. (2000) Incorporation of Short-Lived ^{10}Be in a Calcium-Aluminum-Rich Inclusion from the Allende Meteorite. *Science*, **289**, 1334-1337. <https://doi.org/10.1126/science.289.5483.1334>
- [14] Leya, I., Wieler, R. and Halliday, A.N. (2003) The Predictable Collateral Consequences of Nucleosynthesis by Spallation Reactions in the Early Solar System. *Astrophysical Journal*, **594**, 605-616. <https://doi.org/10.1086/376795>
- [15] Duprat, J. and Tatischeff, V. (2008) On Non-Thermal Nucleosynthesis of Short-Lived Radionuclides in the Early Solar System. *New Astronomy Reviews*, **52**, 463-466. <https://doi.org/10.1016/j.newar.2008.06.016>
- [16] Shu, F.H., Shang, H. and Lee, T. (1996) Toward an Astrophysical Theory of Chondrites. *Science*, **271**, 1545-1552. <https://doi.org/10.1126/science.271.5255.1545>
- [17] Shu, F.H., Shang, H., Glassgold, A.E. and Lee, T. (1997) X-Rays and Fluctuating X-Winds from Protostars. *Science*, **277**, 1475-1479. <https://doi.org/10.1126/science.277.5331.1475>
- [18] Shu, F.H., Shang, H., Glassgold, A.E. and Lee, T. (2001) The Origin of Chondrules and Refractory Inclusions in Chondritic Meteorites. *Astrophysical Journal*, **548**, 1029-1050. <https://doi.org/10.1086/319018>
- [19] Shu, F.H., Shang, H., Glassgold, A.E. and Rehm, K.E. (1998) Protostellar Cosmic Rays and Extinct Radioactivities in Meteorites. *Astrophysical Journal*, **506**, 898-912. <https://doi.org/10.1086/306284>
- [20] Calvet, N., Briceno, B., Hernandez, J., Hoyer, S., Hartmann, L., Sicila, Megeath, S.T. and D'Alessio, P. (2005) Disk Evolution in the Orion OB1 Association. *Astronomical Journal*, **129**, 935-946. <https://doi.org/10.1086/426910>
- [21] Ward-Thompson, D. (1996) The Formation and Evolution of Low Mass Protostars. *Astrophysics & Space Science*, **239**, 151-170. <https://doi.org/10.1007/BF00653775>
- [22] Reedy, R.C. and Marti, K. (1991) Solar-Cosmic-Ray Fluxes during the Last 10 Million Years. In: Sonnet, C.P., Giampapa, M.S. and Mathews, M.S., Eds., *The Sun in Time*, University of Arizona Press, Tucson, 260-287.
- [23] Lodders, K. (2003) Solar System Abundances and Condensation Temperatures of the Elements. *The Astrophysical Journal*, **591**, 1220-1247. <https://doi.org/10.1086/375492>
- [24] Sisterson, J., *et al.* (1997) Measurement of Proton Production Cross Sections of ^{10}Be and ^{26}Al from Elements Found in Lunar Rocks. *Nuclear Instruments and Methods in Physics Research Section B: Beam Interactions with Materials and Atoms*, **123**, 324-329. [https://doi.org/10.1016/S0168-583X\(96\)00409-0](https://doi.org/10.1016/S0168-583X(96)00409-0)
- [25] Gounelle, M., Shu, F.H., Shang, H., Glassgold, A.E., Rehm, K.E. and Lee, T. (2006) The Irradiation Origin of Beryllium Radioisotopes and Other Short-Lived Radionuclides. *The Astrophysical Journal*, **640**, 1163-1189. <https://doi.org/10.1086/500309>